ABRAHAMS, S. C. & MARSH, P. (1987). *Acta Cryst.* A43, 265–269.

ABRAMOWITZ, M. & STEGUN, I. A. (1964). *Handbook of Mathematical Functions.* Washington: US Government Printing Office.

ALLISON, J. D., COTTON, F. A., POWELL, G. L. & WALTON, R. A. (1984). *Inorg. Chem.* 23, 159–164.

BAU, R., CARROLL, W. E., TELLER, R. G. & KOETZLE, T. F. (1977). *J. Am. Chem. Soc.* 99, 3872–3874.

BECKER, P. J. & COPPENS, P. (1974). *Acta Cryst.* A30, 129–147; 148–153.

BUSING, W. R., MARTIN, K. O. & LEVY, H. A. (1973). *J. Appl. Cryst.* 6, 309–346.

EMGE, T. J., KOETZLE, T. F., BRUNO, J. W. & CAULTON, K. G. (1984). *Inorg. Chem.* 23, 4012–4017.

Enraf–Nonius CAD-4 Operations Manual (1982). Enraf–Nonius, Delft, The Netherlands.

GINSBERG, A. P. (1968). *J. Chem. Soc. Chem. Commun.* pp. 857–858.

GREEN, M. A., HUFFMAN, J. C. & CAULTON, K. G. (1981). *J. Am. Chem. Soc.* 103, 695–696.

GREEN, M. A., HUFFMAN, J. C. & CAULTON, K. G. (1982). *J. Am. Chem. Soc.* 104, 2319–2320.

GREEN, M. A., HUFFMAN, J. C., CAULTON, K. G., RYBAK, W. K. & ZIOLKOWSKI, J. J. (1981). *J. Organomet. Chem.* 218, C39–C43.

HOWARD, J. A. K., MEAD, K. A. & SPENCER, J. C. (1983). *Acta Cryst.* C39, 555–559.

International Tables for X-ray Crystallography (1974). Vol. IV. Birmingham: Kynoch Press. (Present distributor Kluwer Academic Publishers, Dordrecht.)

ISCC–NBS Centroid Color Charts (1964). Supplement to NBS Circular 553. Washington: US Government Printing Office.

LUNDGREN, J.-O., KVICK, Å., KARPPINEN, M., LIMINGA, R. & ABRAHAMS, S. C. (1984). *J. Chem. Phys.* 80, 423–430.

POUGET, J. P., SHIRANE, G., BECHGAARD, K. & FABRE, J. M. (1983). *Phys. Rev. B,* 27, 5203–5206.

RINDORF, G., SOLING, H. & THORUP, N. (1984). *Acta Cryst.* C40, 1137–1139.

SCHERINGER, C. (1986). *Acta Cryst.* A42, 356–362.

SCHOMAKER, V. & TRUEBLOOD, K. N. (1968). *Acta Cryst.* B24, 63–76.

WEBER, K. (1969). *Acta Cryst.* B25, 1174–1178.

YAMANAKA, T., TAKEUCHI, Y. & TOKONAMI, M. (1984). *Acta Cryst.* B40, 96–102.

Steric and Electronic Effects on the Structural Parameters of the Dianions $[M_6C(CO)_{15}]^{2-}$ (M = Co, Rh). An Accurate Analysis

By VINCENZO G. ALBANO, DARIO BRAGA* AND FABRIZIA GREPIONI

Dipartimento di Chimica 'G. Ciamician', Universita' di Bologna, Via F. Selmi 2, 40126 Bologna, Italy

Abstract

The structures of the carbido-carbonyl cluster species $[N(C_2H_5)_4]_2[Co_6C(CO)_{15}]$ and $[PPh_4]_2[Rh_6C(CO)_{15}]$ are examined and compared with the results of the previous determinations of the two anions as their isomorphous salts of $[N(CH_2Ph)(CH_3)_3]^+$. A 'sliding effect', similar to that observed on passing from isotropic to anisotropic refinement of the C- and O-atom thermal parameters of terminally bound CO groups, is found to occur for μ_2-bridging CO ligands. $M-M$ bonds within the trigonal prismatic cores of the two species are shown to be significantly affected by changes in the crystal packing, and to depend strongly on the interplay of steric and electronic factors such as CO···CO nonbonding intra- and intermolecular interactions, and bonding M–CO and M–C(carbide) interactions. Crystal data: bis(tetraethylammonium) μ_6-carbido-nona-μ_2-carbonyl-hexacarbonyl-*triprismo*-hexacobaltate(2–), $[N(C_2H_5)_4]_2[Co_6C(CO)_{15}]$, M_r = 1046·3, monoclinic, $P2_1/n$, a = 8·890 (2), b = 22·790 (10), c = 20·545 (6) Å, β = 96·00 (1)°, U =

4139·72 Å³, Z = 4, D_x = 1·68 g cm⁻³, λ(Mo $K\alpha$) = 0·71069 Å, μ = 23·14 cm⁻¹, $F(000)$ = 2112, R = 0·060 for 5929 observed reflections; bis(tetraphenylphosphonium) μ_6-carbido-nona-μ_2-carbonyl-hexacarbonyl-*triprismo*-hexarhodate(2–), $[PPh_4]_2[Rh_6C(CO)_{15}]$, M_r = 1728·4, triclinic, $P\bar{1}$, a = 14·784 (8), b = 18·796 (13), c = 11·339 (7) Å, α = 96·50 (5), β = 90·78 (5), γ = 86·35 (5)°, U = 3124·23 Å³, Z = 2, D_x = 1·84 g cm⁻³, λ(Mo $K\alpha$) = 0·71069 Å, μ = 22·30 cm⁻¹, $F(000)$ = 1688, R = 0·052 for 5582 observed reflections.

Introduction

There is an increasing awareness that a better understanding of the relationships between metal–metal, metal–ligand and ligand–ligand interactions (whether bonding or nonbonding) in transition-metal clusters can be gained if more accurate and reliable structural information is available. The problem is not trivial and it has recently been shown that systematic errors are made, even in the evaluation of some of the most basic structural parameters (such as M–C and C–O bond lengths of terminally bound CO groups), if the

* To whom correspondence should be addressed.

appropriate refinement model is not employed (Braga & Koetzle, 1987). What is more, it has been demonstrated that, even if large and accurate data sets are available, the mean-square displacement amplitudes ('thermal parameters') obtained for the light atoms in room-temperature or low-temperature X-ray studies are heavily contaminated by bonding electron density contributions (Braga & Koetzle, 1988). Metal—metal bonds, on the other hand, show significant variability which depends primarily upon the presence of bridging ligands, but which also shows more subtle relationships with intermolecular and intramolecular interactions (Colton & McCormick, 1980; Braga & Grepioni, 1987; Lauher, 1986).

The aim of this paper is essentially twofold: on one side the dependence on the refinement model ('sliding effect') of the kind observed for terminally bound CO ligands is examined in the case of μ_2-bridging CO's; on the other side metal—metal bonds are analyzed with respect to both intra- and intermolecular nonbonding interactions. The effect of the presence of bridging CO ligands on the M—M distances is also discussed.

The two dianions $[M_6C(CO)_{15}]^{2-}$ ($M = $ Co, Rh), which possess a trigonal prismatic metal-atom framework, were selected for this study. These species not only possess an unusually large number of bridging ligands (see below) with respect to the vast majority of neutral and anionic transition-metal clusters, but can also be easily prepared and crystallized with different counterions. Moreover, both species are precursors of a large variety of new metal clusters, some of which are of high nuclearity, so that a detailed knowledge of their stereogeometries goes beyond the pure analysis of subtle structural effects and may offer new insights into the whole structural chemistry of the carbide clusters of Co and Rh.
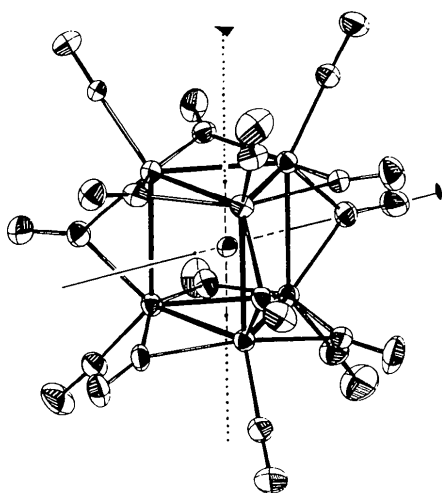
Both species were previously subjected to single-crystal X-ray characterizations and their structures fully described and reported as their $|N(CH_2Ph)$-$(CH_3)_3|^+$ salts in the monoclinic space group $C2/c$ (Martinengo, Strumolo, Chini, Albano & Braga, 1985; Albano, Sansoni, Chini & Martinengo, 1973). The two species were found to be isostructural and their crystals isomorphous with the dianions possessing C_2 crystallographic symmetry (see Fig. 1). The fifteen CO's are regularly distributed with six in terminal positions on each prism vertex, and nine in bridging positions spanning all the polyhedron edges; their idealized symmetry is D_{3h}.

We have now been able to carry out an investigation of the crystal structures of both species obtained with different counterions {$[N(C_2H_5)_4]^+$, for $M = $ Co (1a) and $[PPh_4]^+$ for $M = $ Rh (2a)} affording two new and more accurate data sets well suited for the purposes of this work. Unfortunately, crystallization of isomorphous crystals using the same cations was not achieved. Nonetheless, both dianions lie in general positions in the unit cells, so that the two redeterminations offer a unique opportunity for studying not only the occurrence of a 'sliding effect' on a large number of independent μ_2-CO's (nine) but also the effect of changes in the structural environments on the metal-atom frameworks and ligand coverages.

Experimental

Crystal data and details of measurements for the two new structural characterizations are summarized in Table 1. All atomic coordinates from the full data set refinements have been deposited.* In the following only some salient structural features will be described, with attention mainly focused on the differences observed between the present and earlier structural determinations. The reader seeking details of the preparative routes of these species should refer to the earlier reports. Atomic scattering factors were taken from *International Tables for X-ray Crystallography* (1974). Computer program used: *SHELX*76 (Sheldrick, 1976).

Sliding effect on bridging CO ligands

As mentioned above the C atoms of terminally bound CO groups 'slide' towards the O atoms, along the M—C—O vectors, on simply passing from isotropic to anisotropic refinement of the light-atom positions (Braga & Koetzle, 1987). The differences in bond

Fig. 1. *ORTEP* (Johnson, 1965) drawing of the anion $[M_6C(CO)_{15}]^{2-}$ showing the idealized D_{3h} symmetry (dotted line) and the crystallographic twofold axis (solid line).

Table 1. *Crystal data and details of measurements for (1a) and (2a)*

	(1a)	(2a)
Formula	$C_{32}H_{40}Co_6N_2O_{15}$	$C_{64}H_{40}O_{15}P_2Rh_6$
M_r	1046.3	1728.4
Crystal size (mm)	0.12 × 0.10 × 0.15	0.14 × 0.15 × 0.15
System	Monoclinic	Triclinic
Space group	$P2_1/n$	$P\bar{1}$
a (Å)	8.890 (2)	14.784 (8)
b (Å)	22.790 (10)	18.796 (13)
c (Å)	20.545 (6)	11.339 (7)
α (°)	—	96.50 (5)
β (°)	96.00 (1)	90.78 (5)
γ (°)	—	86.35 (5)
U (Å³)	4139.72	3124.23
Z	4	2
$F(000)$	2112	1688
D_x (g cm⁻³)	1.68	1.84
λ(Mo $K\alpha$) (Å)	0.71069	0.71069
μ(Mo $K\alpha$) (cm⁻¹)	23.14	22.30
Diffractometer used	CAD-4	CAD-4
Scan mode	$\omega/2\theta$	$\omega/2\theta$
θ range (°)	2.5–33	2.5–25
ω-scan width (°)	0.75	0.70
Requested counting $\sigma(I)/I$	0.01	0.01
Prescan rate (min⁻¹)	4	5
Prescan acceptance $\sigma(I)/I$	0.5	0.5
Maximum scan time (s)	180	140
Octants explored in reciprocal space	±h, +k, +l*	±h, ±k, +l
Measured reflections	8540	7232
Unique observed reflections used in the refinement	5929	5582
Absorption correction,† min. and max. values	0.40, 1.00	0.98, 1.00
R, wR,‡ S	0.060, 0.062, 0.776	0.052, 0.056, 1.474
k, g	0.915, 0.009	1.243, 0.001
$(\Delta/\sigma)_{max}$	0.10	0.10
$(\Delta\rho)_{max}$, $(\Delta\rho)_{min}$ (e Å⁻³)	1.10, −1.52	0.78, −0.90

* Equivalent reflections ±h, −k, +l were measured in the range $20 < \theta < 33°$.

† Absorption correction was applied by the method of Walker & Stuart (1983).

‡ $wR = \Sigma[(F_o - F_c)w^{1/2}]/\Sigma(F_o w^{1/2})$, where $w = k/[\sigma^2(F) + |g||F_2|]$.

Table 2. *Comparison of average M–C and C–O bond lengths (Å) determined using isotropic and anisotropic models*

Compound (1a)

	Iso-tropic	Aniso-tropic	Δ	Iso-tropic	Aniso-tropic	Δ	Aniso-tropic
$(\sin\theta/\lambda)_{max}$ (Å⁻¹)	0.48			0.77			0.48–0.77
N_{obs} [$I_o > 2\sigma(I_o)$]	2853			5929			3076
N_{var}	467	617		467	617		617
R, wR* (%)	7.3,8.2	5.6,5.8		8.0,8.9	6.0,6.2		3.9,3.7
Co–C_t	1.70(1)	1.75(1)	0.05	1.74(1)	1.77(1)	0.03	1.77(1)
C_t–O_t	1.19(2)	1.14(1)	−0.05	1.17(1)	1.13(1)	−0.04	1.14(2)
Co–C_b triangular faces	1.93(2)	1.97(2)	0.04	1.96(1)	1.97(1)	0.01	1.97(2)
C_b–O_b triangular faces	1.21(2)	1.16(1)	−0.05	1.18(1)	1.16(1)	−0.02	1.16(1)
Co–C_b square faces	1.88(1)	1.90(1)	0.02	1.90(1)	1.91(1)	0.01	1.91(1)
C_b–O_b square faces	1.21(2)	1.18(1)	−0.03	1.17(1)	1.17(1)	0.00	1.17(1)

Compound (2a)

	Iso-tropic	Aniso-tropic	Δ	Iso-tropic	Aniso-tropic	Δ
$(\sin\theta/\lambda)_{max}$ (Å⁻¹)	0.48			0.60		
N_{obs} [$I_o > 2\sigma(I_o)$]	3999			5582		
N_{var}	470	617		470	617	
R, wR* (%)	5.2,4.9	4.7,4.4		5.9,5.3	5.2,5.6	
Rh–C_t	1.86(2)	1.89(2)	0.03	1.86(2)	1.89(2)	0.03
C_t–O_t	1.14(2)	1.13(2)	−0.01	1.14(2)	1.13(2)	−0.01
Rh–C_b triangular faces	2.09(1)	2.10(1)	0.01	2.09(1)	2.10(1)	0.01
C_b–O_b triangular faces	1.18(2)	1.17(2)	−0.01	1.18(2)	1.16(2)	−0.02
Rh–C_b square faces	2.00(1)	2.02(2)	0.02	2.00(2)	2.02(1)	0.02
C_b–O_b square faces	1.21(2)	1.19(2)	−0.02	1.21(1)	1.19(2)	−0.02

* See Table 1.

lengths are of the order of 0.02–0.05 Å and, though close to the experimental errors, they are systematic, invariably leading to underestimation of M–C and overestimation of C–O distances if isotropic refinement is used for the C and O atoms. It should be emphasized that this latter model is very often employed in metal cluster crystallography because of the large number of structural parameters and (often) the paucity of the available data. In such a way correlations between M–C and C–O structural parameters and information derived from other techniques (such as IR bond-stretching frequencies) or comparison among classes of related species become almost meaningless. We can now prove that μ_2-bridging CO's behave very much in the same way as terminal ligands, although the 'sliding effect' appears to be slightly less pronounced. A comparison between average M–C and C–O bond lengths for both terminal and bridging CO's (the latter ones grouped in two sets of chemically independent ligands), determined by using isotropic and anisotropic refinement models, is reported in Table 2 for (1a) and (2a). A much larger data set [$(\sin\theta/\lambda)_{max}$ = 0.77 Å⁻¹] was obtained for (1a) than for (2a), so that a 'high-order' refinement, though carried out on data

collected at room temperature, could also be attempted for the former (see below). It should be mentioned, at this stage, that corrections for rigid-body motion (Schomaker & Trueblood, 1968) had almost no effect on the structural parameters listed in Table 2, so that uncorrected data are reported. The possibility of internal molecular motion (non-rigid-body contribution) was not checked and cannot be ruled out at present.

Table 2 allows the following considerations:

(i) There is a marked 'sliding effect' on the terminal CO ligands which depends on the limiting value of $(\sin\theta/\lambda)_{max}$. This effect is similar to that found for the species previously examined [$Co_6C(CO)_{13}^{2-}$, $Ir_4(CO)_{11}(SCN)^-$, $HCo_6(CO)_{15}^-$] (Braga & Koetzle, 1987).

(ii) Bridging CO's in both (1a) and (2a) show similar behaviour, yielding longer M–C and shorter C–O bond distances on passing from isotropic to anisotropic refinement (the M–C–M angle varies accordingly).

(iii) The two nonequivalent sets of bridging ligands (basal and interbasal ones) behave very much in the same way.

(iv) The effect decreases with increasing resolution of the data sets. It should be observed, however, that, while the difference between the two refinement models is almost cancelled for the bridging ligands when the largest data sets are employed [$(\sin\theta/\lambda)_{max}$ = 0.77 and 0.60 Å⁻¹ for (1a) and (2a), respectively], coincidence is not achieved for the terminal ligands.

(v) The 'sliding effect' appears to be slightly less pronounced when $M = Rh$ than when $M = Co$, although the former data set is smaller.

(vi) In the case of (1a) a refinement carried out on high-order reflections only [rather arbitrarily selected within the ($\sin\theta/\lambda$) range 0·48–0·77 Å^{-1}] could also be attempted. As can be seen from Table 2, the results are almost identical to those obtained with the full data set anisotropic refinement.

Altogether these observations lend further support to the idea that the 'sliding effect' reflects the large anisotropy of the electron density distribution around the C atoms of metal-bound CO molecules. The decrease of the differences between the two structural models observed on passing from terminal to bridging ligands can be taken as indicative that the electron density distribution for the latter bonding mode is somewhat 'less aspherical' than for the former one. Taking speculations based on so small differences for what they are worth, it should be noted that this behaviour is in keeping with the greater π acidity of μ_2-CO's with respect to terminal CO's, which leads to increased population of the π^* orbitals around the C atoms upon formation of μ_2-bridges. It can be anticipated that μ_3-CO's, which, as shown by their IR stretching frequences, undergo more extensive metal-to-ligand back-donation than the other two types of coordination, should exhibit a further reduction of the 'sliding effect' on passing from isotropic to anisotropic refinement. Unfortunately, there are no available cases in the literature on which this hypothesis can be tested.

It should be emphasized that the different behaviour shown by CO ligands in their different bonding modes renders extremely difficult a straight correlation of their structural parameters with information from IR spectroscopy such as bond-length/bond-strength/stretching-frequency comparisons. Only very large (and often unfeasable) data sets or neutron diffraction studies might allow work in this direction to be carried out with confidence. Nonetheless, it seems worth suggesting that, whenever a reasonable level of accuracy is sought, the largest θ range should be covered and light atoms treated anisotropically even in the presence of low N_{obs}/N_{var} ratios.

Effects of bridging CO ligands on M–M bond lengths

A careful investigation of the structural features of (1a) and (2a) also allows some insights into the relationships between the size of the metal-atom polyhedra (in terms of M–M bond lengths) and the surrounding ligand envelopes, which have been shown to have a strong influence on the structural parameters of the metal core (Johnson & Benfield, 1981). As mentioned above the peculiarity of the $[M_6C(CO)_{15}]^{2-}$ species arises from the fact that all edges are spanned by bridging CO ligands, a rather exceptional feature in metal cluster compounds, so that the effect of these ligands on the M–M bond distances should be more marked. Table 3 shows a comparison of the average

Table 3. *Comparison of relevant structural parameters* (Å) *between* (1a) *and* (2a) *and the octahedral species* $[M_6C(CO)_{13}]^{2-}$ (M = Co, Rh)

	$[Co_6C-(CO)_{15}]^{2-}$ (1a)	$[Co_6C-(CO)_{13}]^{2-}$	$[Rh_6C-(CO)_{15}]^{2-}$ (2a)	$[Rh_6C-(CO)_{13}]^{2-}$
M–M(bridged)	2·537 (1)* 2·573 (1)†	2·483 (1)	2·772 (1)* 2·819 (1)†	2·773 (1)
M–M(unbridged)		2·750 (1)		3·039 (1)
M–M(average)	2·549 (1)	2·639 (1)	2·790 (1)	2·907 (1)
M–C(carbide)	1·75 (2)	1·87 (2)	2·13 (2)	2·05 (2)
r_C‡	0·68	0·55	0·74	0·60
C···C§	2·64* 2·65†	3·00	2·91* 2·88†	3·07
O···O§	3·95* 3·83†	4·21	3·73* 3·55†	4·05

* Prism triangular faces.
† Prism square faces.
‡ Apparent C-atom radius, r_C = (M–C) – $\overline{(M-M)}/2$.
§ Intramolecular next-neighbour contacts.

values in the two dianions. Average bond lengths are also reported for the octahedral species $[M_6C(CO)_{13}]^{2-}$ [M = Co (Albano, Braga & Martinengo, 1986) and M = Rh (Albano, Braga & Martinengo, 1981)], which will be used later in the discussion.

Co–Co bond lengths are as expected shorter than the corresponding Rh–Rh ones, but it should be noted that CO-bridged bonds in the related carbide species reported in Table 3 show Rh–Rh bonds of comparable length in (2a) and $[Rh_6C(CO)_{13}]^{2-}$, while Co–Co bonds appear to be shorter in $[Co_6C(CO)_{13}]^{2-}$ than in the prismatic core of (1a). The distances for this latter species appear to be longer also with respect to the values observed in other families of Co clusters containing bridging ligands such as $[Co_4(CO)_{12}]$ (Wei, 1966; Carre', Cotton & Frenz, 1976) and its derivatives (bridged Co–Co bonds are usually found within the range 2·46–2·48 Å) or $[Co_6(CO)_{15}]^{2-}$ (Albano, Chini & Scatturin, 1968), whose μ_2-bridged Co–Co bonds average 2·47 Å.

The reason for this discrepancy must be found in the subtle interplay of several factors such as intramolecular-ligand, metal–ligand and metal–metal interactions. As can be seen in Table 3, the average next-neighbour CO···CO contact distances (calculated for both C···C and O···O contacts) reach a minimum in (1a) being shorter than in the Rh prism and in both Co- and Rh-octahedral species. It has already been shown that nonbonding interactions play a key role in establishing the more stable stereogeometry for the family of octahedral carbide species (Albano, Braga, Grepioni, Della Pergola, Garlaschelli & Fumagalli, 1988) and are responsible, for instance, for the remarkable structural differences observed between the $[M_6C(CO)_{13}]^{2-}$ species mentioned above (Albano, Braga & Martinengo, 1981, 1986) or among the members of the family of $[M_4(CO)_{12}]$ derivatives (Braga & Grepioni, 1987).

Taking a value of 2·48 Å as a rough estimate of the 'optimum' CO-bridged Co–Co bond length, it appears

that a prismatic polyhedron with bonds around that length would have either to 'force' the surrounding CO ligands below acceptable limits of their van der Waals interactions or 'loosen' bonding interactions with the ligands by lengthening the Co—C bonds. In this context, it is worth noting that, while Co—Co bond lengths are distributed over large ranges (see Table 3), Co—C(CO) bond distances are found to be almost identical in their mean values on going from the prismatic to the octahedral species [Co—C$_t$ 1·77 (1), 1·76 (2), Co—C$_b$ 1·95 (1), 1·93 (2) Å, respectively]. In conclusion, the comparison between the prism/octahedron pairs nicely supports the suggestion, put forward earlier, that $M-M$ bonding is sacrificed first when ligand—ligand repulsions became dominant or the efficiency of metal—ligand interactions is at risk. This observation agrees with the thermochemical evidence of stronger M—CO than $M-M$ interactions in metal carbonyl clusters (Connor, 1980).

It may also be argued that the interstitial C(carbide) atom plays some role in determining the optimum size of the surrounding metal cage. This does seem to be an important point: although the apparent radius of C in the octahedral Co species, despite the presence of CO-bridged bonds of 'normal' length, is much smaller (0·55 Å) than within the prismatic cavity (0·68 Å), the deformations of the former cage allow a longer average Co—C distance [1·87 versus 1·75 Å]. Shorter Co—Co bonds (of the order of 2·48 Å) within the prismatic core would therefore lead to a probably unacceptable reduction of the Co—C(carbide) distances. In summary, it seems reasonable to regard the structure of (1a) as the result of a difficult compromise between several nonconverging factors: nonbonding CO···CO and bonding Co—C(carbide) interactions requiring a larger metal frame, and Co—Co and Co—(μ_2-CO)—Co interactions requiring a somewhat smaller metal frame.

Effect of crystal packing on $M-M$ bond lengths

This last section is aimed at recognition of those molecular features that are more affected by the crystal packing and at the investigation of the relationship between crystallographically imposed symmetry (site symmetry) and molecular symmetry (idealized symmetry). For the reasons mentioned above the family of [M_6C(CO)$_{15}$]$^{2-}$ species offers a good opportunity in this direction. The effect of variations in the packing environments is expected to show up in those structural parameters more related to flexible molecular parts affording mainly indications on the relative strength of the bonds and rigidity of bond angles. It should be recalled, at this stage, that methods based on this kind of approach are widely applied to isomorphous crystals of organic compounds (Bernstein & Hagler, 1978; Bar & Bernstein, 1984). In those systems, however, most information comes from

Table 4. *Comparison of M—M bond distances* (Å) [M = Co, Rh] *between* (1a) *and* (1b), *and between* (2a) *and* (2b)

	Triangular faces		Square faces	
	M—M range	M̄—M̄	M—M range	M̄—M̄
(1a)|N(C₂H₅)₄|₂|Co₆C(CO)₁₅|.* space group P2₁/n, Z = 4, site symmetry C₁	2·529–2·535(1) 2·529–2·552(1)	2·531 2·541	2·564–2·586(1)	2·570
(1b)|N(CH₂Ph)Me₃|₂|Co₆C(CO)₁₅|, space group C2/c, Z = 4, site symmetry C₂	2·533–2·541(1)	2·537	2·574–2·578(2)	2·576
(2a)|PPh₄|₂|Rh₆C(CO)₁₅|.* space group P1̄, Z = 2, site symmetry C₁	2·769–2·792(1) 2·758–2·770(1)	2·777 2·765	2·813–2·826(1)	2·819
(2b)|N(CH₂Ph)Me₃|₂|Rh₆C(CO)₁₅|, space group C2/c, Z = 4, site symmetry C₂	2·772–2·783(2)	2·776	2·817–2·817(2)	2·817

* $M-M$ bond lengths within the two crystallographically independent triangular faces were averaged separately.

differences in torsion angles, while bonds (mainly C—C bonds) are usually found to be substantially rigid. The situation is somewhat reversed in the systems discussed here because bonds, especially $M-M$ bonds, show the largest structural variability. This is surprising at first sight in that $M-M$ bonds are usually believed to build up the 'hard' metallic cores.

Table 4 reports a comparison of $M-M$ bond distances between the two pairs of prismatic species [X]$_2$[M_6C(CO)$_{15}$] [M = Co, X = N(C₂H₅)₄, (1a); M = Co, X = N(CH₂Ph)(CH₃)₃, (1b); M = Rh, X = PPh₄ (2a); M = Rh, X = N(CH₂Ph)(CH₃)₃, (2b)]. More than the average values, which are almost identical for each of the two pairs, differences can be appreciated in the ranges spanned by individual $M-M$ bond lengths (grouped in Table 4 according to molecular symmetry). Although the precision of the individual values is very high (e.s.d.'s never exceed 0·002 Å) the differences shown by equivalent sets of values are marked. One striking systematic difference on passing from (1b) and (2b), which lie around a crystallographic twofold axis, to (1a) and (2a), which lie in general positions, is found in the prism triangular faces. As a matter of fact both (1a) and (2a) have triangular faces whose $M-M$ bonds not only differ in the spanned ranges, but also in their mean values, showing that one face is smaller than the opposite one [2·531, 2·541 for (1a), 2·765, 2·777 Å for (2a)]. These differences appear to be significant, being one order of magnitude larger than the e.s.d.'s of each value. It is interesting to observe that equivalence of the two triangular faces is otherwise imposed by crystallographic symmetry in (1b) and (2b) [M̄—M̄ 2·537 in (1b), 2·776 Å in (2b)]. The effect of the 'loss' of the C_2 symmetry is also evidenced by the interbasal $M-M$ bond lengths which span a much larger range in (1a) and (2a) than in (1b) and (2b) [2·564–2·586 (1), 2·574–2·578 (2); 2·813–2·826 (1), 2·817–2·817 (2) Å, respectively]. These structural effects are ascribed to the different packings allowed by the [N(CH₂Ph)(CH₃)₃]$^+$ cations in (1b) and

(2b) with respect to $[N(C_2H_5)_4]^+$ in (1a) and $[PPh_4]^+$ in (2a), these latter cations establishing nonequivalent sets of electrostatic and van der Waals interactions with the respective anions. Unfortunately, beside the recognition of the different interactions between the anions and the surrounding cations, there is no simple rationalization of the causes of the observed shrinkage of one triangular face with respect to the other in (1a) and (2a). Nonetheless, these observations strengthen the idea that the inner metal-atom polyhedra have to be regarded as the 'soft' cores of these species, capable of adapting themselves to the steric and electronic demands of both the ligands packed around the core and the surrounding molecules.

Concluding remarks

We have shown that there is a clear borderline between the knowledge of the structural parameters concerning the ligands and those related to the metal cores in transition-metal clusters. $M—M$ bonds and angles can be determined with great precision, but appear to be related to relatively adaptable parts of the molecules, which can be easily affected by small changes in both ligand coverages and crystal packing. On the other hand, the parameters related to metal–ligand (or ligand–ligand) interactions and which contain more 'chemical information', are known with reduced precision and are significantly dependent on experimental limitations and refinement strategies.

References

ALBANO, V. G., BRAGA, D., GREPIONI, F., DELLA PERGOLA, R., GARLASCHELLI, L. & FUMAGALLI, A. (1988). *J. Chem. Soc. Dalton Trans.* In the press.
ALBANO, V. G., BRAGA, D. & MARTINENGO, S. (1981). *J. Chem. Soc. Dalton Trans.* pp. 717–720.
ALBANO, V. G., BRAGA, D. & MARTINENGO, S. (1986). *J. Chem. Soc. Dalton Trans.* pp. 981–984.
ALBANO, V. G., CHINI, P. & SCATTURIN, V. (1968). *J. Organomet. Chem.* 15, 423–432.
ALBANO, V. G., SANSONI, M., CHINI, P. & MARTINENGO, S. (1973). *J. Chem. Soc. Dalton Trans.* pp. 651–655.
BAR, I. & BERNSTEIN, J. (1984). *J. Phys. Chem.* 88, 243–248.
BERNSTEIN, J. & HAGLER, A. T. (1978). *J. Am. Chem. Soc.* 100, 673–681.
BRAGA, D. & GREPIONI, F. (1987). *J. Organomet. Chem.* 336, C9–C12.
BRAGA, D. & KOETZLE, T. F. (1987). *J. Chem. Soc. Chem. Commun.* pp. 144–146.
BRAGA, D. & KOETZLE, T. F. (1988). *Acta Cryst.* B44, 151–155.
CARRE', F. H., COTTON, F. A. & FRENZ, B. A. (1976). *Inorg. Chem.* 15, 380–387.
COLTON, R. & McCORMICK, M. J. (1980). *Coord. Chem. Rev.* 31, 1–52.
CONNOR, J. A. (1980). *Transition Metal Clusters*, edited by B. F. G. JOHNSON, pp. 345–389. New York: John Wiley.
International Tables for X-ray Crystallography (1974). Vol. IV. Birmingham: Kynoch Press. (Present distributor Kluwer Academic Publishers, Dordrecht.)
JOHNSON, B. F. G. & BENFIELD, R. E. (1981). *Inorg. Organomet. Stereochem.* 12, 253–335, and references therein.
JOHNSON, C. K. (1965). *ORTEP.* Report ORNL-3794. Oak Ridge National Laboratory, Tennessee, USA.
LAUHER, J. W. (1986). *J. Am. Chem. Soc.* 108, 1521–1531.
MARTINENGO, S., STRUMOLO, D., CHINI, P., ALBANO, V. G. & BRAGA, D. (1985). *J. Chem. Soc. Dalton Trans.* pp. 35–41.
SCHOMAKER, V. & TRUEBLOOD, K. N. (1968). *Acta Cryst.* B24, 63–76.
SHELDRICK, G. M. (1976). *SHELX76.* Program for crystal structure determination. Univ. of Cambridge, England.
WALKER, N. & STUART, D. (1983). *Acta Cryst.* A39, 158–166.
WEI, C. H. (1966). *Inorg. Chem.* 8, 2384–2397.

Deformation Density Studies of Tetramethylthiuram Disulfide and Tetraethylthiuram Disulfide

BY YU WANG* AND J. H. LIAO

Department of Chemistry, National Taiwan University, Taipei, Taiwan

Abstract

Two thiuram disulfide compounds, whose room-temperature structures have been reported previously, were studied by X-ray diffraction at low temperature. Tetramethylthiuram disulfide (1), $C_6H_{12}N_2S_4$, $M_r = 240.4$, monoclinic, $C2/c$, $a = 9.524$ (4), $b = 9.911$ (3), $c = 11.795$ (1) Å, $\beta = 99.22$ (1)°, $V = 1099$ Å^3, $Z = 4$, $D_x = 1.47$ g cm^{-3}, $\lambda(Mo\ K\alpha) = 0.71069$ Å, $\mu = 7.7$ cm^{-1}, $T = 138$ K, final $R = 0.031$ for 2881 reflections. Tetraethylthiuram disulfide (2), $C_{10}H_{20}N_2S_4$, $M_r = 296.5$, monoclinic, $P2_1/c$, $a = 10.922$ (3), $b = $

* To whom all correspondence should be addressed.